- Technical Paper -

A SIMULATION-AIDED STUDY ON MICROSTRUCTURE DEVELOPMENT AND DENSIFICATION PROCESS OF CEMENTITIOUS MATERIALS

Guangfeng OU[*1], Seunghyun NA[*2], Tomohisa KAMADA[*3] and Toshiharu KISHI[*4]

ABSTRACT

Numerical simulation (The μic model) is used in this study to unfold the pore structure development of cement as hydration proceeds. It is found conventional modeling technique fails to dynamically trace the microstructure development due to the time-dependent bulk density of C-S-H. Additionally, w/c ratio will affect its densification process. Therefore, a densification model is applied to rationally solve the problem. Furthermore, in view of the limitation of voxel size in the simulation technique, it underscores the significance of a multi-scale interpretation on densification process of C-S-H structure.

Keywords: C-S-H, densification, numerical simulation, time-dependent density

1. INTRODUCTION

The early-age development of pore structure can impose significant influences on the mechanical, transport, and durability properties of cementitious materials. However, the complexity of pore morphology (i.e., porosity, connectivity and tortuosity) and multi-scale nature (which spans several orders) of pore size has exerted much difficulties on characterizing and quantifying the development of pore structure. The original HYMOSTRUC model treated elements of material with fixed properties independent of time [1], and further, the updated multi-scale model divides the pore structure into three levels (<5 nm, 5-100nm and >100nm), in which the packing of C-S-H globules are classified into two groups: loosely-packed outer C-S-H and densely-packed inner C-S-H. The DuCOM model used an expanding cluster model to predict the time-dependent bulk density of hydration products [2]. Whereas, the intrinsic governing mechanism regarding how C-S-H densifies (e.g., how the low-density product and high-density product vary with age, w/c, temperature and drying) is not revealed in these models. The time-dependency of bulk density of C-S-H is rather complicated in reality, which requires a proper understanding and rational description of its densification process. Actually, a realistic densification mechanism should not only be limited to explain the pore structure development, but should also consistently rationalize the hydration kinetics, and the moisture state inside pores. Because all of these processes (hydration kinetics, pore structure development and moisture change) are taking place simultaneously in an interactive and coupled manner.

A dynamic densification process of C-S-H has been implemented by S. Bishnoi to rationally model the hydration kinetics of alite particles using the developed platform $\boldsymbol{\mu ic}$ [3]. In this study, the same densification model is utilized to understand the microstructure development of cement (including Alite, Belite, aluminate phase, ferrite phase, gypsum and impurities). The time-dependent bulk density of C-S-H is implemented in the model. The conventional scheme using constant C-S-H density is also conducted for comparison. The effect of w/c on the densification process is analyzed by comparison with published experimental data. Furthermore, the significant implications of the simulation results, the limitation of current voxel-based characterization method, and a future perspective are discussed.

2. SIMULATION SCHEME

2.1 Outline of $\boldsymbol{\mu ic}$

μic is a modelling framework which has been established to simulate complex particle interaction of hydrating cement pastes by S. Bishnoi [3]. The hydration kinetics and pore structure can be computed in a system with millions of particles. Its flexible and customizable properties also facilitate the simulation of different physical/chemical mechanisms and their evolution process, serving as an ideal tool for understanding more realistic hydration kinetics and pore structure development during hydration.

2.2 Materials

(1) Reactions

The widely-used stoichiometric reactions proposed by Bentz [4] are adopted and lumped as the following equations for simplicity.

$$1.0V_{C_3S} + 1.344H \rightarrow 1.521V_{CSH} + 0.606V_{CH} \quad (1)$$

$$1.0V_{C_2S} + 1.488H \rightarrow 2.077V_{CSH} + 0.191V_{CH} \quad (2)$$

$$1.0V_{OtherPhase} \rightarrow 1.97V_{Crystalline} \quad (3)$$

[*1] Department of Civil Engineering, The University of Tokyo, JCI Student Member

[*2] Institute of Industrial Science, The University of Tokyo, Technical Staff

[*3] Institute of Industrial Science, The University of Tokyo, Assistant Professor

[*4] Institute of Industrial Science, The University of Tokyo, Professor

In which V denotes the volume of each phase (C_3S, C_2S, CSH, CH, crystalline, etc.). H denotes water and subscript "OtherPhase" represents aluminate and aluminoferrite phase. It can be interpreted from Eq. (1) to Eq. (3) that one volume of reacted cement will produce 2.13 volume of hydration products ($\kappa_h = 2.13$), which corresponds well to the generally-accepted range of value [5,6]. The physical properties of these equations are listed in Table 1. Noted that the constant value of C-S-H density is only used in the conventional model scheme, while in the densification model, time-dependent bulk density is expressed by the following Eq. (4) [3]:

$$\frac{d\rho}{dt} = k_{den} \cdot \frac{\rho_{max} - \rho}{\rho_{max} - \rho_{min}} \qquad (4)$$

Eq.(4) can be rephrased as:

$$\rho = (\rho_{max} - \rho_{min}) \cdot \exp\left(\frac{-k_{den} \cdot t}{\rho_{max} - \rho_{min}}\right) \qquad (5)$$

Where, ρ denotes the bulk density of C-S-H. Eq.(4) and Eq. (5) indicate the density will increase from a minimum value ρ_{min} to a maximum value ρ_{max} and its variation rate in time is controlled by a constant parameter k_{den} (g/cm^3/h).

Table 1 Densities of Reactants and Products (g/cm^3)

Scheme	Cement	CH	Other Crystallines	CSH
Conventional	3.15	2.24	3.06	2.12
Densification				ρ_{min} ~ρ_{max}

Note: The values of ρ_{min} and ρ_{max} will be discussed later.

Additionally, two nucleation cases of outer C-S-H products are simulated. Case 1 (termed as homogenous case): outer C-S-H nuclei are set to randomly formed in the pore volumes. Case 2 (termed as heterogenous case): very fine outer C-S-H nuclei is only allowed to be formed as attached on the surface of the particles.

2.3 Modeling Input

(1) Input Kinetics

In this study, nucleation and growth mechanism (a modified form of Avrami Equation [7]) followed by the diffusion controlled mechanism are set as reaction kinetics.

(2) Particle Size Distribution

The distribution of particles simulated in this study caters to the actual particle distribution of cement [5]. One advantage of using μic is that millions of particle numbers can be computed which agrees much with the realistic situation and without much computation cost. In this study, millions of cement particles are simulated. The REV size is 100 μm, and voxel size used to post-process the pore size distribution is 0.25μm. Noted that μic exploits the vector approach that does not depend on the resolution during calculation (i.e., multi-scale information is preserved). Voxels are only used when post-processing the pore structure information by a pixel-erosion method to facilitate the computation of millions of particles [7].

(3) Other Modeling Features

Other features like periodic boundary conditions, optimization of the vector approach and customizable reaction conditions can be referred to the literature [7].

3. SIMULATION RESULTS AND DISCUSSION

(1) Homogenous and Heterogenous Nucleation ....

Fig. 1 and Fig. 2 denote the pore structure development during hydration for the homogenous and heterogenous case, respectively. Dark blue phase represents inner C-S-H, which is formed inside the original boundary of particles. Light blue particles represent the outer hydration products (Outer CSH, CH and other crystalline products are integrated together and plotted in light blue for better visualization). Black area is the capillary pores.

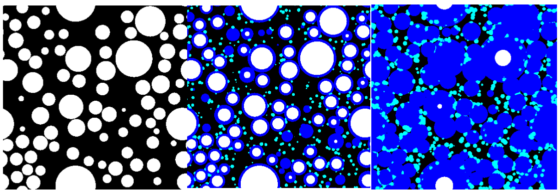

Fig. 1 Homogenous Nucleation of Outer Products (Hydration Degree: 0, 0.72 and 0.85)

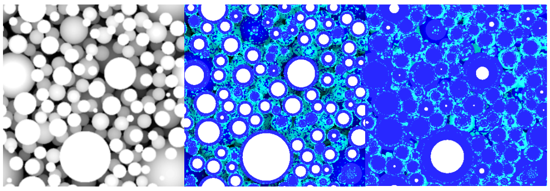

Fig. 2 Heterogenous Nucleation of Outer Products (Hydration Degree: 0, 0.72 and 0.85)

The periodic boundary condition is clearly depicted by aligning figures close to each other, it can be easily seen that the particles on the right boundary of first column of graph actually are the ones on the left boundary of the second, so on and so forth. It can be found that in the homogenous case, outer C-S-H is randomly formed in the capillary pore space, whereas in the heterogenous case, it is closely confined on the surface of particles.

The BSE (Back-scattered electron) experiment results of hydrating cement paste from Ma [5] are plotted in Fig. 3 to compare with the modeling results of pore size distribution for the homogenous case. The hydration degree for cement paste with w/c of 0.40 and 0.50 cured for 60 days are 0.72 and 0.79 respectively, determined experimentally by TGA [5]. The hydration degree in the simulation is defined as the volume of hydrated cement over that of the original cement [7]. Since the BSE technique eliminates the ink-bottle effect encountered by MIP results, such a comparison is more reasonable instead of using MIP results. As shown in Fig. 3, scheme using homogenous nucleation will lead to relatively large deviation for total porosity in the range larger than 0.1 μm.

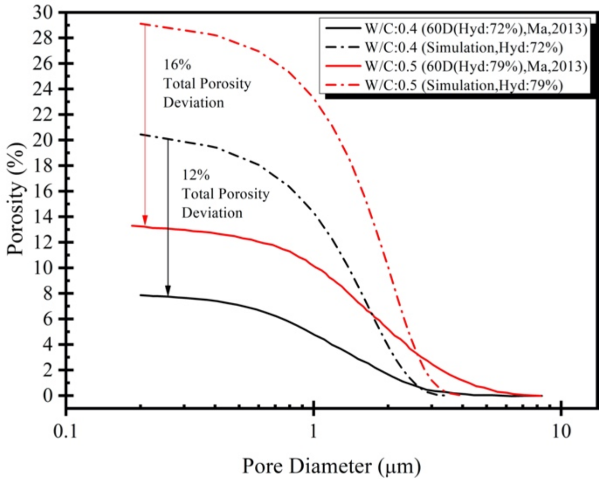

Fig. 3 Porosity Deviation of homogenous case

While the heterogenous case surprisingly leads to much smaller porosity at the same hydration degree, being closer to the experimental results, as shown in Fig. 4. Noted that in both cases, only the nucleation sites are varied (one is randomly formed in the pore space, the other is formed on the surface of particles), other parameters and reaction conditions are all identical.

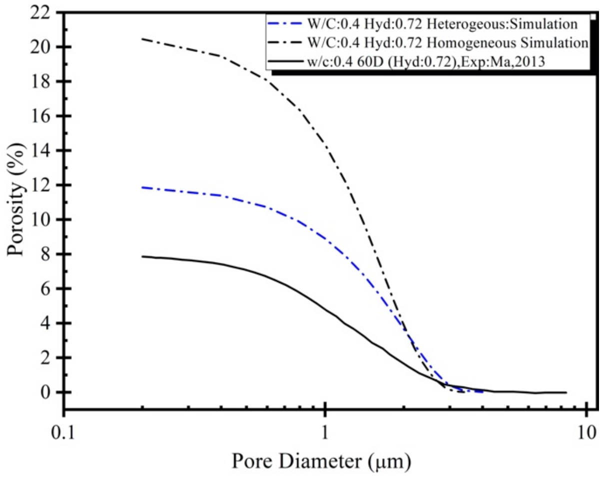

Fig. 4. Comparison in the heterogenous case

A clearer qualitative comparison with both cases under same hydration degree (0.72) can be found from Fig. 5. Deep image technique is used in the heterogenous case to visualize the confined hydration products on the surface (right figure). It can be seen, the thickness of inner hydration products (the dark blue region) is almost the same for both cases, having around several micro-meter. It implies the discrepancy is not due to the inner products.

Quantitative information of the two cases are further plotted in Fig. 6 and Fig. 7 to clarify the reason of those discrepancies. Fig. 6 reveals that each component amount (Cement, CSH, CH and Crystalline) is exactly the same in both cases, signifying the computation is correct.

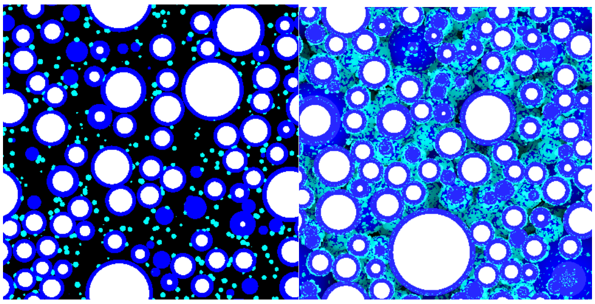

Fig. 5 A two-dimensional slice of homogenous (left) and heterogenous case (right), with hydration degree=0.72

While some discrepancies are found for the pixel number in two cases. As shown in Fig. 7, the voxels of hydration products computed in two cases start to differ from each other after hydration degree reaches around 0.25. Those overestimated volume of hydration products in the heterogenous case explain well the smaller total porosity found in Fig. 4.

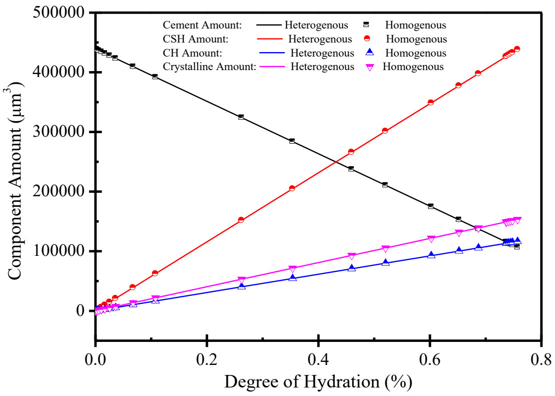

Fig. 6 Amount of chemical component

It is also interesting to know that hydration degree of around 0.25 also closely matches with the time when impingement between particles take place. Therefore, it can be envisaged that when hydration products (mainly the outer CSH) of particles start to impinge with each other, pixels can be easily captured and counted in the homogenous case. While some very fine and tortuous pores (mostly gel pores smaller than 0.1 μm) between hydration products cannot be captured in the heterogenous case due to the pixel-based characterization method for porosity in the model. Pixel size (0.25μm) is too large for many fine pores between hydration products. These pores are not “seen” by the pixel-based method. A schematic diagram is plotted in Fig. 8 to illustrate this process, where red zone represents the pores between particles.

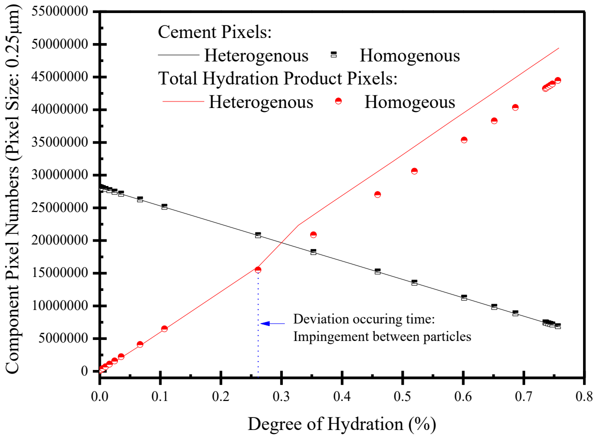

Fig. 7. Pixel numbers of both cases

Fig. 8 (a) Schematic Diagram of particle impingement in homogenous case and (b) heterogenous case

It demonstrates that the realistic development of hydration products should be more analogous to the heterogenous case. The results of conventional simulation scheme (both homogenous and heterogenous) reveal that a constant stoichiometric density of CSH fails to express the pore structure development, since many fine pores within or between hydration products cannot be treated properly. It highlights the importance of a proper description of bulk density of CSH, which varies with time, w/c, temperature and drying condition [10,11]. In the next section, a densification model considering the time-dependent bulk density of C-S-H will be discussed.

(2) The Densification Model

The time-dependent densification process has been successfully used by S. Bishnoi to model the hydration kinetics of alite [3]. The current section aims to figure out how to use this concept to interpret the microstructure development, so that both kinetics and microstructure development can be explained consistently. Herein, a schematic representation is given in Fig. 9.

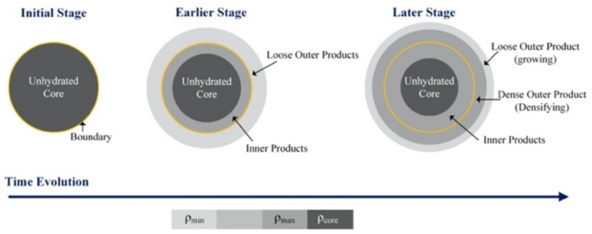

Fig. 9 Schematic diagram of simulated densification

A densification mechanism is proposed as the follows. At the initial stage, unhydrated core of cement is plotted as the darkest grey color, with the orange-colored boundary. At the earlier stage, inner hydration products are formed, along with loose outer products having very low bulk density (ρ_{min}). It leads to a very rapid volume expansion of outer hydration products at earlier age, which also accounts for the deceleration branch in the hydration kinetics [3]. This loosely-packed structure formed in the early age acts as a skeleton (or “scaffold” structure). Then, in the later age, two simultaneous effects will be taking place. Firstly, more outer C-S-H will be formed inside the skeleton (or “scaffold”), which defines a densification process with increasing density. Secondly, more loosely packed C-S-H structure will be formed at the outer rim, causing the volume expansion and occupying more capillary pores. This volume occupation of capillary pore space by hydration products has been widely studied and accepted [8]. Interestingly, the densification process (i.e., increasing bulk density of C-S-H as hydration proceeds) has also been recently proved by the advancement of experiment using ^{1}H NMR [9].

The bulk density of C-S-H will cease to densify when it reaches a defined maximum value ρ_{max}. By defining the time-dependent bulk density of C-S-H, the undetectable volume of fine pores in conventional scheme (see last section) can be taken into account. It should be pointed out that the definition and clear separation of these two simultaneous effects are hard to be applied in $\boldsymbol{\mu ic}$, which needs to define two time-dependent behaviors at the same time, i.e., the densifying outer hydration products and the expanding outer hydration products.

Therefore, in the current model, only one time-dependent bulk density of the whole outer hydration product is considered. The governing equation for this process is given in Eq. (4). Tentatively, in this study we use values given in literature [3], $\rho_{max} = 2.0\ g/cm^3$ and K_{den} is a constant value of 0.007g/cm^3/h. Then, ρ_{min} is computed in an iterative way until satisfactory matches with the experimental results are found.

After optimizing the model, it is found that when ρ_{min} equals to ~0.65 g/cm^3 (excluding any evaporable water), the modeling results are in good agreement with the experiment results for 60 Days of hydration, as shown in Fig. 10. The output of model at steps with identical hydration degree as experiments are used for direct comparison. The modeling results demonstrate the feasibility and applicability of adopting such a densification concept to describe the microstructure development of cement.

Additionally, different water-to-cement ratios (w/c=0.3, 0.4 and 0.5) are also modeled to elucidate the effect. The same computation methodology as aforementioned is utilized. The computation results are shown in Fig. 10. Results for all w/c cases are consistent with the experimental results. The optimized values for ρ_{min} are 0.82 g/cm^3, 0.65 g/cm^3 and 0.57 g/cm^3 for w/c equal to 0.3, 0.4 and 0.5, respectively. That is to say, at lower w/c ratio, a higher initial bulk density ρ_{min} is found.

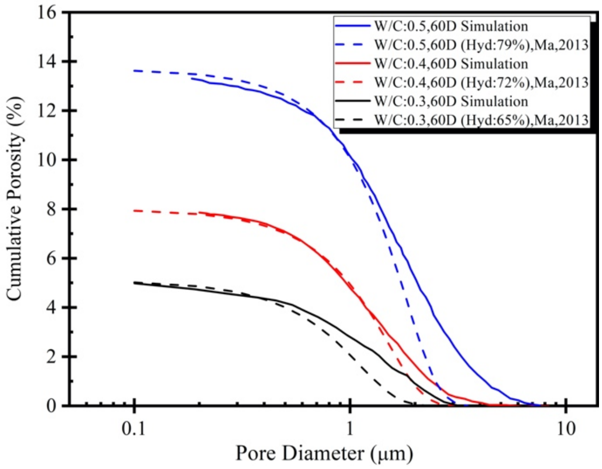

Fig.10 Computed pore size distribution with varied w/c using densification model (Age=60 Days)

Importantly, the simulation results indicate the densification process is not only age-dependent, but also greatly relies on w/c. Varied w/c will lead to different densification effect. If we view it from another perspective by keeping the initial bulk density values ρ_{min} the same in three w/c cases and attempt to search the densification rate k_{den} for all three w/c cases, one can readily conclude that a lower w/c requires much higher densification rate. It is noteworthy that this mechanism corresponds well to the concept of two types of C-S-H proposed by Jennings [10,11], which states that under a low w/c situation, the ratio of HD CSH (high-density) C-S-H to LD (low-density) CSH is higher than that in high w/c situation. Recent studies [12] on micromechanics analysis also supports that HD C-S-H tends to be formed in restricted space and LD C-S-H in more open space.

Noted that the density ρ_{min} described here represents the bulk density excluding any evaporable water present in pores. After converting to saturated bulk densities, they will be ~1.53 g/cm^3, 1.42 g/cm^3 and 1.37 g/cm^3 for w/c equal to 0.3, 0.4 and 0.5 respectively. These values are smaller than the value of saturated low-density C-S-H in Jennings' model [10,11], i.e., ~1.93 g/cm^3 (converted from d-dried density to saturated density). But it is reasonable that at very early age, more loosely-packed C-S-H than relatively mature C-S-H can be formed, e.g., as evidenced by studies using TEM image for OPC cement paste cured for 12 hours [13].

(3) Limitation of Pixel-based Method

It is difficult for pixel-based method to characterize the multi-scale properties of pore structure, which spans over several orders of size (from nm to μm scale). Even though the size of a pixel is chosen as 0.1 μm, most of the fine gel pores having nano-meter size cannot be considered using conventional computation method. One solution is that using high-resolution numerical model that simulates nanoparticles in nm-scale (or even starting from molecular level) to predict the thermal-hygro-mechanical behavior of the material in a full-scale (from nm up to μm). But, obviously, such a model is of very high computation cost and not available up to now. An alternative is to interpret the material properties using multi-scale model. Cementitious materials possess heterogeneities at different scales. In a multi-scale approach, the heterogenous nature in a smaller scale is upscaled as a homogenized response in a larger scale. And thus, varied behaviors in different scales can be bridged and predicted. The key point of multi-scale approach is to obtain accurate and rational constitutive responses when upscaling, which can truly express the behavior of the materials. In this study, the densification concept is a way to homogenize the nano-scale porosity within C-S-H as a time-dependent bulk density, so that its development and pore size distribution in micrometer scale can be simulated properly.

(4) Implications and Future Perspectives

Due to the complexity of the densification process, which is related to age (or time), w/c, temperature and drying conditions, etc., it is of great importance to conduct further study to elucidate its mechanism. A mathematical model (or constitutive law) to express this process should be formulated properly, so that a multi-scale approach can be implemented. In this way, it can consistently explain experimental results in varied scale (MIP, Nitrogen adsorption, SANS and NMR, etc).

The advancement of understanding on C-S-H requires the aid of all aforementioned experimental techniques and also, more importantly, it requires a proper interpretation of these experimental results. For example, when nitrogen adsorptions tests are conducted on cement paste specimen with same w/c=0.5, varied interpretations can lead to contrasted conclusions [5,14], which hinders the proper use of these experimental data into the model. Experimental results from Ma [5] is plotted in Fig. 11. It was concluded in his study that porosity from 3 nm to 100 nm detected by nitrogen adsorption tests is decreasing as curing time increases, and such pores are categorized into small capillary pores. The porosity of these capillary pores is decreasing due to the volume occupation of more hydration products. Whereas in Zeng's study [14] (Fig. 12), it can be found that the porosity of pores smaller than 4 nm increases as hydration time proceeds, while pores in the range >4 nm demonstrates an unclear trend against hydration time. Such discrepancies between researches imply that a more comprehensive and deeper understanding on densification process is required, which provides insight on a more rational classification of varied types of pores and their evolution patterns. It also serves as fundamental and key problems for shrinkage-related problems, because the moisture state and transport properties greatly associate with pore morphologies.

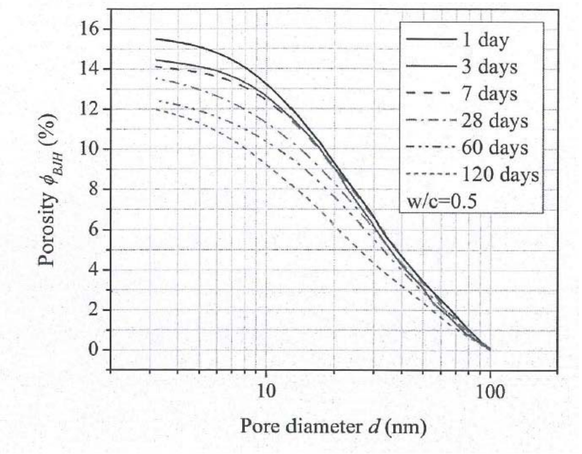

Fig. 11. Porosity of cement paste (w/c=0.5) tested in Nitrogen Adsorption Test [5].

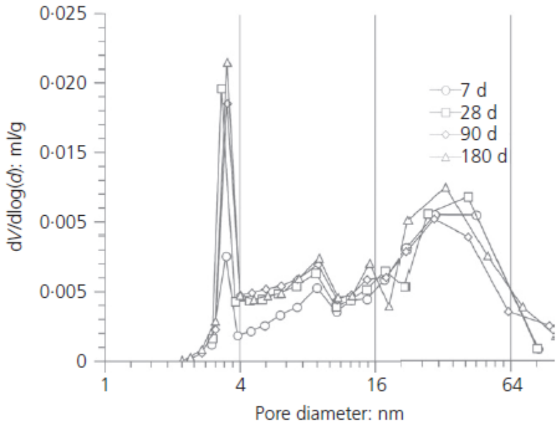

Fig. 12. Derivative plot of porosity of cement paste (w/c=0.5) tested in Nitrogen Adsorption Test [14].

3. CONCLUSIONS

(1) The study shows that conventional modeling technique fails to model the pore structure development due to the missed volume of fine pores contained in the C-S-H product.

(2) Simulation indicates outer C-S-H nuclei is prone to nucleate in a heterogenous way, which is confined on the surface of the particles.

(3) A densification model is successfully implemented to trace the dynamic change of time-dependent bulk density of C-S-H. The effect of w/c is also studied, which implies an intensified densification effect in low w/c case.

(4) The limitation of pixel-based characterization method for pore structure is discussed, followed by a discussion on important implications and future perspective.

REFERENCES

[1] S.J. LOKHORST, K. van BREUGEL.” From Microstructural development towards prediction of macro stresses in hardening concrete”, Thermal Cracking in Concrete at Early Ages., E & FN SPON, 1994, pp. 71-78.

[2] K. MAEKAWA, T. ISHIDA, T. KISHI. “Multi-scale modeling of structural concrete”, Taylor & Francis, 2009.

[3] S. BISHNOI, K.L. SCRIVENER. “Studying nucleation and growth kinetics of alite hydration using *μic*”, Cem. Con. Res., 2009, pp. 849-860.

[4] D.P. BENTZ. “Three-dimensional computer simulation of portland cement hydration and microstructure development”, *J. Am. Ceram.*, 1997, 80(1), pp. 3-21.

[5] H.Y. MA. “Multi-scale modeling of the microstructure and transport properties of contemporary concrete”, HKUST, 2013, PhD Thesis.

[6] J., SANAHUJA, L. DORMIEUX, G., CHANVILLARD. “Modelling elasticity of a hydrating cement paste.”, Cem. Con. Res., 2007, 37 (10), pp. 1427-1439.

[7] S. BISHNOI, “Vector Modelling of. Hydrating Cement Microstructure and Kinetics”, EPFL, 2008, PhD Thesis.

[8] H.F.W. TAYLOR, Cement Chemistry (2nd ed.), Thomas Telford, Lon- don, U.K., 1997.

[9] A.C.A. Muller, K. L. Scrivener, A. M. Gajewicz, P.J. McDonald, “Densification of C-S-H Measured by ^{1}H NMR Relaxometry”, J. Phys. Chem. Lett., 2013, 117, 403-412.

[10] H. JENNINGS, “A model for the microstructure of calcium silicate hydrate in cement paste”, Cem. Con. Res., 2000, 30 (1) pp. 101-116.

[11] H. JENNINGS, “Refinements to colloid model of C-S-H in cement: CM-II”, Cem. Con. Res., 2008, 3 (38), pp. 275-289.

[12] V. SMILAUER, Z. BITTNAR, “Microstructure-based micromechanical prediction of elastic properties in hydrating cement paste”, Cem. Con. Res., 2006, 36, pp. 1708-1718.

[13] P.C. MATHUR, “Study of cementitious materials using transmission electron microscopy”, Doctoral Thesis, École Polytechnique Fédérale de Lausanne, 2007.

[14] Q. ZENG, K. LI, F. CHONG, “Pore structure of. cement pastes through NAD and MIP analysis”, Adv. Cem. Res. 2016, 28 (1), pp. 23-32